Energy of the quasi-free electron in argon, krypton and xenon

Xianbo Shi [a,b], Luxi Li [a,b], C. M. Evans [a,b], G. L. Findley [c]

[a] *Department of Chemistry and Biochemistry, Queens College – CUNY, 65-30 Kissena Blvd, Flushing, NY 11367*
[b] *Department of Chemistry, The Graduate Center – CUNY, New York, NY 10016*
[c] *Department of Chemistry, University of Louisiana at Monroe, Monroe, LA 71209*

Abstract

Recent field ionization measurements of various high-n molecular Rydberg states doped into argon, krypton and xenon perturbers are presented as a function of perturber number density up to the density of the triple point liquid. These data are modeled to within ±0.3% of experiment on both critical and noncritical isotherms using a new theoretical treatment that includes: (i) the polarization of the perturber by the dopant cation, (ii) the polarization of the perturber by the quasi-free electron that arises from field ionization of the dopant, and (iii) the kinetic energy of the quasi-free electron. The polarization terms are determined by a standard statistical mechanical treatment. However, the kinetic energy of the quasi-free electron is calculated within a new local Wigner-Seitz model that contains only one adjustable parameter. This treatment provides an accurate model of the energy of the bottom of the conduction band (V_0) in argon, krypton and xenon from the dilute gas up to the density of the triple point liquid, on both critical and noncritical isotherms.

Key words: supercritical fluids, quasi-free electron, effective range theory
PACS: 72.40.+w, 51.50.+v, 31.70.-f

The use of supercritical fluids in environmental remediation, in the treatment of high-level hazardous wastes and in tailoring chemical reactions for specific product yields necessitates a better understanding of density and temperature effects on the properties of neutral and charged species solvated in these fluids. We have recently studied the perturber induced shift $\Delta_{\rm D}(\rho_{\rm P})$ of dopant ionization energy – and the quasi-free electron energy $V_0(\rho_{\rm P})$ – in the rare gases Ar [1–3], Kr [1,4] and Xe [5] at noncritical temperatures and on an isotherm near the critical isotherm (i.e., $T_r \equiv T/T_c \leq 1.01$). These data show a clear deviation near the critical density along the critical isotherm of the perturber. Accurate treatment of $V_0(\rho_{\rm P})$ led to the development of a new local Wigner-Seitz model [1–5], which requires only a single adjustable parameter to give a fit that is within ±0.3% of experiment. This paper presents a short review of these results.

Experimental information on the dopants and perturbers used in these studies and the procedures used to ensure homogeneous mixing of samples in the gas handling system have been described previously [1–6]. The details of the experimental sample cell, along with procedures for the determination of a dopant molecule field ionization spectrum from two photoionization spectra measured at different electric fields, have also been published previously [1–5] and will not be repeated here.

The quasi-free electron energy $V_0(\rho_{\rm P})$ in a dense perturbing gas can be extracted from $\Delta_{\rm D}(\rho_{\rm P})$, which is determined from field ionization studies, using [1–5]

$$V_0(\rho_{\rm P}) = \Delta_{\rm D}(\rho_{\rm P}) - P_+(\rho_{\rm P})\,, \qquad (1)$$

where $P_+(\rho_{\rm P})$ is the ensemble average dopant ionic core/perturber polarization energy, and $\rho_{\rm P}$ is the perturber number density. $P_+(\rho_{\rm P})$ is calculated from a standard statistical mechanical treatment via [1–5]

$$P_+(\rho_{\rm P}) = -4\pi\rho_{\rm P}\int_0^\infty g_{\rm PD}(r)\; w_+(r)\; r^2 dr\,. \qquad (2)$$

In eq. (2) $g_{\rm PD}(r)$ is the perturber/dopant radial distribution function, and $w_+(r)$ is the perturber/ion interaction potential [1–5]. Since $w_+(r)$ incorporates induced dipole interactions in the perturbing medium, the perturber/perturber radial distribution function $g_{\rm PP}(r)$ is also involved in determining $P_+(\rho_{\rm P})$. The radial distribution functions $g_{\rm PD}(r)$ and $g_{\rm PP}(r)$ are computed from the coupled Percus-Yevick integro-differential equation method [1,7], with a Lennard-Jones 6-12 potential used for the perturber/perturber interactions [1,5] and a modified Stockmeyer potential employed for the dopant/perturber interactions [1,5]. $V_0(\rho_{\rm P})$ extracted from eq. (1) is presented in Fig. 1 for Ar [1–3],

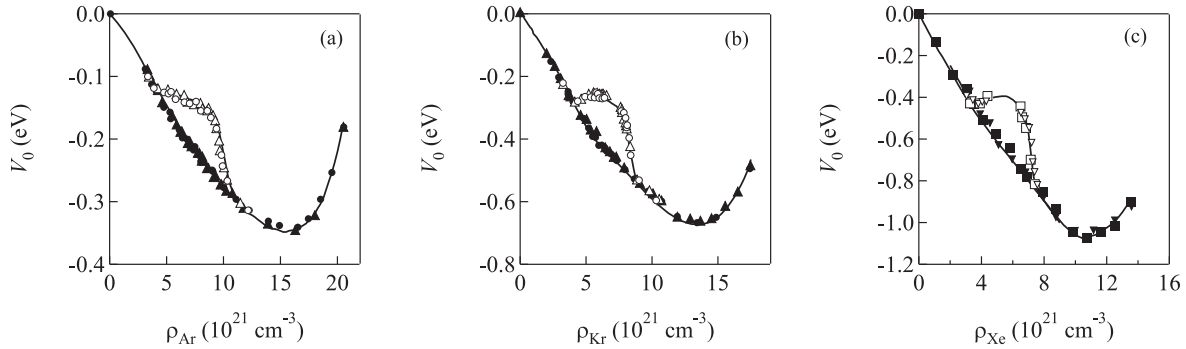

Fig. 1. The quasi-free electron energy $V_0(\rho_P)$ for (a) Ar [1–3], (b) Kr [1,4] and (c) Xe [5] at noncritical temperatures (solid markers) and on an isotherm near the critical isotherm of the perturber (open markers), extracted from eq. (1), plotted as a function of perturber number density ρ_P. (▲ [1], △ [2,4]) represent data extracted from CH_3I field ionization, (● [1], ○ [3,4]) are data obtained from C_2H_5I field ionization, (■ [5], □ [5]) are data determined from N,N-dimethylaniline field ionization, and (▼ [5], ▽ [5]) represent data from trimethylamine field ionization. The solid lines are a calculation of $V_0(\rho_P)$ from eq. (6) with the parameters given in Table 1. See text for discussion.

Kr [1,4] and Xe [5]. These data show a striking change in $V_0(\rho_P)$ near the critical density on an isotherm near the critical isotherm of the perturber.

The quasi-free electron energy $V_0(\rho_P)$ in a dense gas can be written as a sum of three terms [1–5]

$$V_0(\rho_P) = P_-(\rho_P) + E_k(\rho_P) + \frac{3}{2}k_BT\,, \qquad (3)$$

where $P_-(\rho_P)$ is the average polarization energy of the pertuber interacting with the quasi-free electron, $E_k(\rho_P)$ is the zero-point kinetic energy of the electron, and $3k_BT/2$ is the thermal energy of the electron. The average polarization energy $P_-(\rho_P)$ can be calculated in a manner similar to the average cation/perturber polarization energy [i.e., eq. (2)], namely [1–5]

$$P_-(\rho_P) = -4\pi\rho_P \int_0^\infty g_{PP}(r)\; w_-(r)\; r^2 dr\,, \qquad (4)$$

where $w_-(r)$ is the electron/perturber interaction potential originally proposed by Lekner [1,8].

The local density of atoms $\rho_P(r)$ at any radial distance from a given perturber atom can be determined from [1] $\rho_P(r) = \rho_P\; g_{PP}(r)$. The local Wigner-Seitz radius r_ℓ, which represents one half the average spacing between atoms in the first solvent shell, is given by [1]

$$r_\ell = \sqrt[3]{\frac{3}{4\;\pi\;g_{max}\;\rho_P}}\,, \qquad (5)$$

where g_{max} is the maximum of the perturber/perturber radial distribution function. The maximum distance of the optical electron/perturber interaction in the first solvent shell is, therefore, given by the difference between the local Wigner-Seitz radius r_ℓ and a hard-sphere radius defined by the absolute value of the zero-kinetic-energy electron scattering length A of the perturber at low density. Assuming that the electron/perturber interaction in the first solvent shell dominates the zero-point kinetic energy and that this interaction can be treated simply as a particle in a spherical well, the quasi-free electron energy $V_0(\rho_P)$ becomes

$$V_0(\rho_P) = P_-(\rho_P) + \frac{\hbar^2\,a^2}{2\,m_e}\frac{1}{(r_\ell - |A|)^2} + \frac{3}{2}k_BT\,, \qquad (6)$$

where a is a unitless adjustable parameter determined by the best fit to the experimental data, $\hbar$ is the reduced Planck constant, and m_e is the electron mass. The solid lines shown in Fig. 1 represent eq. (6) with the parameters given in Table 1. This simple approximation models the data to within ±0.3% of experiment, and shows the correct critical point behavior. (The critical point behavior arises from r_ℓ, since r_ℓ decreases near the critical density along the critical isotherm due to density fluctuations.)

A more formal treatment of $V_0(\rho_P)$ begins within the Springett, Jortner and Cohen (SJC) model [9] modified by the local Wigner-Seitz radius [1]. Within this treatment [1,9], $V_0(\rho_P)$ is obtained from the solution to the one-electron Schrödinger equation under the assumption that the potential $V(r)$ is spherical with an average translational symmetry of $V(r) = V(r + 2r_\ell)$. The local Wigner-Seitz model assumes that $V(r) = P_-(\rho_P) + V_a(r)$, where $P_-(\rho_P)$ is a constant for any given density and $V_a(r)$ is a simple hard-sphere potential [i.e., $V_a(r) = 0$ for $r > |A|$ and $V_a(r) = \infty$ for $r \le |A|$]. Under these assumptions, the solution to the Schrödinger equation is

$$\psi_0 = \frac{1}{r}\sin\left[k_0(r - |A|) + \delta\right]\,, \qquad (7)$$

where the wave-vector k_0 is determined from the solution to the boundary condition equation [1]

$$\tan\left[k_0(r_\ell - |A|) + \delta\right] - k_0\; r_\ell = 0\,, \qquad (8)$$

and δ is a phase shift arising from the polarization of perturbers close to the optical electron. This phase shift, which is density dependent, is necessary since $P_-(\rho_P)$ only accounts for the average polarization of perturbers at a dis-

Table 1
The zero-kinetic-energy electron scattering length A [6] and the unitless parameter a used in eq. (6) to obtain the solid lines in Fig. 1.

Perturber	A (Å)	a
Ar	-0.82 ± 0.02	0.329 ± 0.003
Kr	-1.60 ± 0.02	0.133 ± 0.004
Xe	-3.24 ± 0.04	0.0745 ± 0.0006

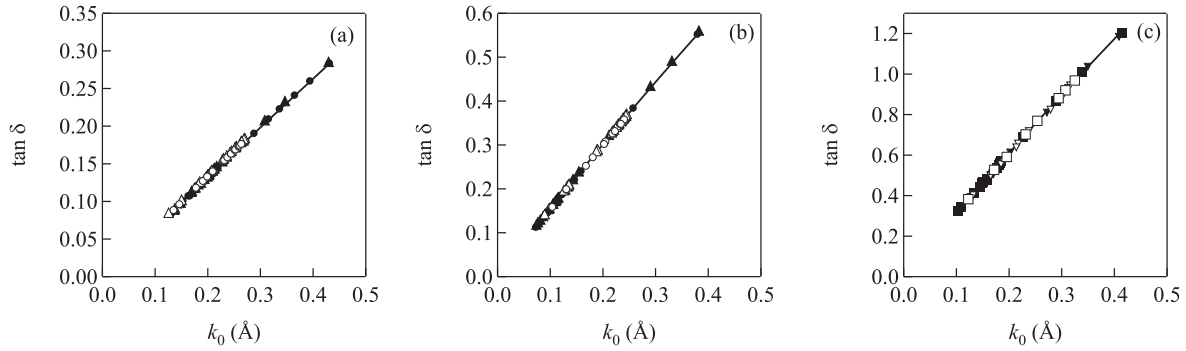

Fig. 2. The tangent of the phase shift δ for (a) Ar, (b) Kr, and (c) Xe at noncritical temperatures (solid markers) and on an isotherm near the critical isotherm of the perturber (open markers), plotted as a function of the wave-vector k_0. See the legend to Fig. 1 for the definition of the markers. The solid lines are a nonlinear least squares analysis of eq. (10). See text for discussion.

tance $r \gg r_\ell$ [8]. [We should note here that determining k_0 from eq. (8) using a standard bracketing and bisection method [10] inadvertently converges on the discontinuties in eq. (8) rather than the actual solutions. However, since eq. (6) holds for all of the data presented here, this inappropriate solution still yields correct numerical values of k_0 for a constant value of δ [1–5], since $k_0(r_\ell - |A|)$ is a constant.] Thus, within the local Wigner-Seitz model, the energy of the quasi-free electron $V_0(\rho_{\rm P})$ is given by

$$V_0(\rho_{\rm P}) = P_-(\rho_{\rm P}) + \frac{\hbar^2\, k_0^2}{2\, m_e} + \frac{3}{2} k_B T\,, \qquad (9)$$

after the inclusion of the thermal kinetic energy of the quasi-free electron.

The phase shift for low kinetic energy electron/atom scattering from effective range theory is given by [11]

$$\tan\delta = A_1 k_0 + A_2 k_0^2 + O(k_0^3)\,. \qquad (10)$$

For very low density atomic gases, $A_1 = -A$ and $A_2 \propto -\alpha_{\rm P}$, where $\alpha_{\rm P}$ is the polarizability of the perturber. Fig. 2 shows $\tan\delta$, calculated from the experimental data of Fig. 1 using eqs. (8)-(9), plotted as a function of the wave-vector k_0 for Ar, Kr and Xe. Clearly, the experimental data obtained at noncritical temperatures and those obtained near the critical isotherm fall on a single curve. Nonlinear least squares analyses of eq. (10) are provided as solid lines in Fig. 2, and the coefficients are summarized in Table 2. The A_1 coefficent obtained from this least squares analysis is close to the zero-kinetic-energy electron scattering length A (cf. Table 1). The coefficient A_2 shows a similar trend to the polarizability of the rare gas atoms (i.e., $\alpha_{\rm Ar} < \alpha_{\rm Kr} < \alpha_{\rm Xe}$). Moreover, the error in the least squares analysis is small. Thus, the phase shift has the correct form of an electron/atom scattering phase shift from effective range theory. The differences between A_1 and A_2 observed in the experimental data as compared to the effective range theory values probably arise from many-body interactions in dense gases, and we are currently working to develop an understanding of these relationships for A_1 and A_2. We are also attempting to develop a theoretical understanding of the parameter a in eq. (6) within the local Wigner-Seitz model. Finally, we are in the process of extending the local Wigner-Seitz model to dense CH_4 [12] at noncritical temperatures and along the critical isotherm.

Table 2
Coefficients A_1 and A_2 obtained from the nonlinear least squares analysis of eq. (10).

Perturber	A_1 (Å)	A_2 (Å^2)
Ar	0.670 ± 0.001	-0.031 ± 0.005
Kr	1.58 ± 0.00	-0.300 ± 0.008
Xe	3.16 ± 0.01	-0.577 ± 0.006

The experimental measurements reported here were performed at the University of Wisconsin Synchrotron Radiation Center (NSF DMR-0537588). This work was supported by grants from the Petroleum Research Fund, from the Professional Staff Congress - City University of New York, and from the Louisiana Board of Regents Support Fund.

References

[1] C.M. Evans, G.L. Findley, Phys. Rev. A 72 (2005) 022717, and references therein.
[2] C.M. Evans, G.L. Findley, Chem. Phys. Lett. 410 (2005) 242.
[3] C.M. Evans, G.L. Findley, J. Phys. B: At. Mol. Opt. Phys. 38 (2005) L269.
[4] Luxi Li, C.M. Evans, G.L. Findley, J. Phys. Chem. A 109 (2005) 10683.
[5] Xianbo Shi, Luxi Li, C.M. Evans, G.L. Findley, Chem. Phys. Lett. 432 (2006) 62.
[6] C. M. Evans, J. D. Scott, G. L. Findley, Rec. Res. Dev. Chem. Phys. 3 (2002) 351.
[7] E.W. Grundke, D. Henderson, R.D. Murphy, Can. J. Phys. 51 (1973) 1216.
[8] J. Lekner, Phys. Rev. 158 (1967) 130.
[9] B.E. Springett, J. Jortner, M.H. Cohen, J. Chem. Phys. 48 (1968) 2720.
[10] W.H. Press, S.A. Teukolsky, W.T. Vetterling, B.P. Flannery, *Numerical Recipes in Fortran: The Art of Scientific Computing* (Cambridge Univ. Press, Cambridge, 2005) p. 354.
[11] T.F. O'Malley, Phys. Rev. 130 (1963) 1020.
[12] Xianbo Shi, Luxi Li, C.M. Evans and G.L. Findley, in preparation.